

Atmospheric Chemistry of 2-Pentanone and 2-Heptanone

ROGER ATKINSON,^{*,†}
ERNESTO C. TUAZON, AND
SARA M. ASCHMANN

*Air Pollution Research Center, University of California,
Riverside, California 92521*

2-Pentanone and 2-heptanone are available for commercial use, which will lead to their possible release into the atmosphere where they are expected to primarily react with the hydroxyl (OH) radical and contribute to the formation of photochemical air pollution in urban and regional areas. We have studied the kinetics and products of the gas-phase reactions of the OH radical with 2-pentanone and 2-heptanone at 298 ± 2 K and atmospheric pressure of air. Using a relative rate method, rate constants for the reactions of the OH radical with 2-pentanone and 2-heptanone of $(4.56 \pm 0.30) \times 10^{-12}$ and $(1.17 \pm 0.11) \times 10^{-11}$ cm³ molecule⁻¹ s⁻¹, respectively, were obtained, where the indicated errors are two least-squares standard deviations and do not include the ~10–15% uncertainties associated with the rate constant for the reference compound cyclohexane. Reaction products were analyzed by gas chromatography, in situ Fourier transform infrared spectroscopy, and in situ atmospheric pressure ionization tandem mass spectrometry (API-MS). The products identified and quantified were (with their molar yields) as follows: from 2-pentanone, formaldehyde, 1.03 ± 0.10 ; acetaldehyde, 0.51 ± 0.11 ; propanal, 0.19 ± 0.03 ; 2,4-pentanedione, 0.12 ± 0.03 ; and molecular weight 147 organic nitrates, 0.12 ± 0.04 ; and from 2-heptanone, formaldehyde, 0.38 ± 0.08 ; acetaldehyde, ~0.05; propanal, ~0.05; butanal, 0.07 ± 0.01 ; pentanal, 0.09 ± 0.01 ; and molecular weight 175 organic nitrates, 0.18 ± 0.05 . API-MS analyses also showed the formation of products of molecular weight 128 and 144 from 2-heptanone, anticipated to be C₇-dicarbonyl(s) and C₇-hydroxydicarbonyl(s), respectively. While 94 ± 13% of the reaction pathways of the 2-pentanone reaction are accounted for, it appears that a substantial fraction (>50%) of the initially formed alkoxy radicals from 2-heptanone undergo isomerization to form products which could not be quantified.

Introduction

2-Pentanone [methyl propyl ketone, CH₃C(O)CH₂CH₂CH₃] and 2-heptanone [methyl amyl ketone, CH₃C(O)CH₂CH₂CH₂CH₂CH₃] are available for commercial use, which will lead to their possible release into the atmosphere where they will undergo photolysis and/or chemical reaction (1, 2) and hence contribute to the formation of photochemical air pollution in urban and regional areas (3). On the basis of our current

understanding of the atmospheric chemistry of these and other similar ketones (1, 2), it is anticipated that the most important tropospheric transformation process for these two ketones is by reaction with the hydroxyl (OH) radical. While rate constants have been measured for the reactions of the OH radical with 2-pentanone (4–6) and 2-heptanone (5), to date no data have been reported concerning the products and mechanisms of these reactions.

Accordingly, we have investigated the products and mechanisms of the gas-phase reactions of 2-pentanone and 2-heptanone with the OH radical. There are some discrepancies between the absolute rate study of Wallington and Kurylo (5) and relative rate studies carried out in this laboratory (4, 6) concerning the rate constants for the reactions of the OH radical with 2- and 3-pentanone and 2-hexanone. We have therefore measured rate constants for the reactions of the OH radical with 2-pentanone and 2-heptanone as part of the present study.

Experimental Methods

Kinetic Studies. The experimental methods were similar to those we have used previously (7). Experiments were carried out at 298 ± 2 K and 740 Torr total pressure of purified air (at ~5% relative humidity) in a 7900-L all-Teflon chamber equipped with two parallel banks of blacklamps for irradiation and a Teflon-coated fan to ensure rapid mixing of reactants during their introduction into the chamber. In the relative rate method used, the relative disappearance rates of the ketones and a reference organic, whose OH radical reaction rate constant is reliably known, were measured in the presence of OH radicals. Provided that the ketones and reference organic were removed solely by reaction with OH radicals, then

$$\ln \left\{ \frac{[\text{ketone}]_{t_0}}{[\text{ketone}]_t} \right\} = \frac{k_1}{k_2} \ln \left\{ \frac{[\text{reference organic}]_{t_0}}{[\text{reference organic}]_t} \right\} \quad (I)$$

where [ketone]_{t₀} and [reference organic]_{t₀} are the concentrations of the ketones and the reference organic at time t₀, [ketone]_t and [reference organic]_t are the corresponding concentrations at time t, and k₁ and k₂ are the rate constants for reactions 1 and 2, respectively:



Hydroxyl radicals were produced by the photolysis of methyl nitrite (CH₃ONO) in air at wavelengths >300 nm (8), and NO was also included in the reactant mixtures to suppress the formation of O₃ and, hence, of NO₃ radicals (8). The initial concentrations of the reactants (in molecule cm⁻³ units) were as follows: CH₃ONO, ~2.4 × 10¹⁴; NO, ~2.4 × 10¹⁴, and the ketones and reference organic, ~2.4 × 10¹³ each. Cyclohexane was used as the reference organic because its OH radical reaction rate constant is similar to those previously reported for 2-pentanone and 2-heptanone (9) and it could be analyzed by gas chromatography using the same sampling and analysis procedures. Irradiations were carried out for 10–45 min at 20% of the maximum light intensity. The concentrations of the ketones and cyclohexane were measured during the reactions by gas chromatography with flame ionization detection (GC-FID). Gas samples of 100 cm³ volume were collected from the chamber onto Tenax-TA solid adsorbent, with subsequent thermal desorption at -225 °C onto a 30-m

* Corresponding author phone: (909)787-4191; fax: (909)787-5004; e-mail: ratkins@mail.ucr.edu.

† Also at the Department of Environmental Sciences and Department of Chemistry, University of California, Riverside.

DB-1701 megabore column held at $-20\text{ }^{\circ}\text{C}$ and then temperature programmed to $200\text{ }^{\circ}\text{C}$ at $8\text{ }^{\circ}\text{C min}^{-1}$.

Product Studies. Experiments were carried out at $298 \pm 2\text{ K}$ and 740 Torr total pressure of air in three reaction chambers. These consisted of (i) a 5870-L evacuable, Teflon-coated chamber containing an in situ multiple reflection optical system interfaced to a Nicolet 7199 Fourier transform infrared (FT-IR) spectrometer and with irradiation provided by a 24-kW xenon arc filtered through a 0.25 in. thick Pyrex pane (to remove wavelengths $<300\text{ nm}$), (ii) a 7900-L Teflon chamber with analysis by GC-FID and combined gas chromatography–mass spectrometry (GC–MS), with irradiation provided by two parallel banks of blacklamps, and (iii) a 7500-L Teflon chamber interfaced to a PE SCIEX API III MS/MS direct air sampling, atmospheric pressure ionization tandem mass spectrometer (API-MS), again with irradiation provided by two parallel banks of blacklamps. All three chambers are fitted with Teflon-coated fans to ensure rapid mixing of reactants during their introduction into the chamber.

Hydroxyl radicals were generated in the presence of NO by the photolysis of methyl nitrite (CH_3ONO) or ethyl nitrite ($\text{C}_2\text{H}_5\text{ONO}$) in air at wavelengths $>300\text{ nm}$ (8, 10), and NO was included in the reactant mixtures to suppress the formation of O_3 and hence of NO_3 radicals (8). Ethyl nitrite was used as the OH radical precursor for the in situ FT-IR analyses of formaldehyde (10) because the photolysis of methyl nitrite leads to the formation of formaldehyde.

Teflon Chamber with Analysis by GC-FID and GC–MS. For the experiments carried out in the 7900-L Teflon chamber (at $\sim 5\%$ relative humidity), the initial reactant concentrations (in molecule cm^{-3} units) were as follows: CH_3ONO , $(2.2\text{--}2.3) \times 10^{14}$; NO, $(2.1\text{--}2.4) \times 10^{14}$; and 2-pentanone or 2-heptanone, $(2.25\text{--}2.46) \times 10^{13}$. Irradiations were carried out at 20% of the maximum light intensity for 15–45 min, resulting in up to 33% and 44% reaction of the initial 2-pentanone or 2-heptanone, respectively. GC-FID analyses of the ketones and their reaction products were carried out as described above, with the DB-1701 megabore column being initially held at -40 or $-60\text{ }^{\circ}\text{C}$ and then temperature programmed to $200\text{ }^{\circ}\text{C}$ at $8\text{ }^{\circ}\text{C min}^{-1}$. Gas samples were also collected from the chamber onto Tenax-TA solid adsorbent for thermal desorption with analysis by GC–MS after preconcentration by an Entech 7000 dehydration preconcentrator, using a 30-m DB-1701 fused silica capillary column in a Hewlett-Packard (HP) 5890 GC interfaced to a HP 5971A mass selective detector operating in the scanning mode. GC-FID response factors for 2-pentanone, 2-heptanone, acetaldehyde, propanal, butanal, pentanal, and 2,4-pentanedione were determined as described previously (11).

Teflon Chamber with Analysis by API-MS. In the experiments with API-MS analyses, the chamber contents were sampled through a 25 mm diameter \times 75 cm length Pyrex tube at $\sim 20\text{ L min}^{-1}$ directly into the API mass spectrometer source. The operation of the API-MS in the MS (scanning) and MS/MS [with collision activated dissociation (CAD)] modes has been described elsewhere (12). Use of the MS/MS mode with CAD allows the “daughter ion” or “parent ion” spectrum of a given ion peak observed in the MS scanning mode to be obtained (12). The positive ion mode was used in these analyses, with protonated water hydrates $[\text{H}_3\text{O}^+(\text{H}_2\text{O})_n]$ being used as the ionizing agent and resulting in the ions that were mass-analyzed being mainly protonated molecular ions ($[\text{M} + \text{H}]^+$) and their protonated homo- and heterodimers (12). The initial concentrations of CH_3ONO , NO, and 2-pentanone or 2-heptanone were $\sim 4.8 \times 10^{13}$ molecule cm^{-3} each, and irradiations were carried out for 10 (2-heptanone) or 15 min (2-pentanone) at 20% of the maximum light intensity.

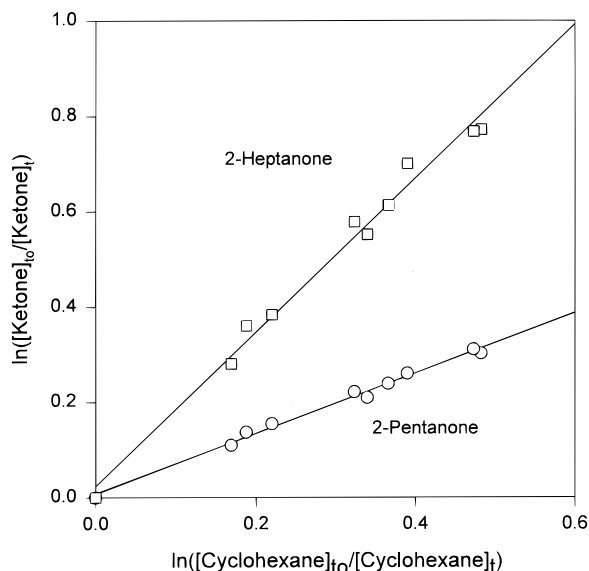


FIGURE 1. Plot of eq 1 for the gas-phase reactions of 2-pentanone and 2-heptanone with the OH radical, using cyclohexane as the reference compound.

Evacuatable Chamber Experiments with FT-IR Analysis. For the experiments carried out in the 5870-L evacuable, Teflon-coated chamber (at $<1\%$ relative humidity), the initial concentrations (in molecule cm^{-3} units) were as follows: CH_3ONO or $\text{C}_2\text{H}_5\text{ONO}$, 2.46×10^{14} ; NO, $(1.72\text{--}1.85) \times 10^{14}$; and 2-pentanone or 2-heptanone, $(2.37\text{--}2.46) \times 10^{14}$. IR spectra of the reaction mixtures were recorded prior to and during irradiation with 64 scans (corresponding to 2.0-min averaging time) per spectrum, a full-width-at-half-maximum resolution of 0.7 cm^{-1} , and a path length of 62.9 m. The mixtures were irradiated intermittently for a number of 4–12-min periods (with total irradiation times of 15–37 min) or for one experiment with 2-heptanone continuously for 15 min, with IR spectra being obtained during the intervening dark periods or (for the continuous irradiation) during the irradiation.

Chemicals. The chemicals used and their stated purities were as follows: cyclohexane (HPLC grade), Fisher Scientific; acetaldehyde (99.5+%), butanal (99%), 2-heptanone (98%), pentanal (99%), 2,4-pentanedione (99+%), 2-pentanone (99+%), and propanal (99+%), Aldrich Chemical Co.; and NO ($\geq 99.0\%$), Matheson Gas Products. Methyl nitrite was prepared as described by Taylor et al. (13), while ethyl nitrite was distilled from a commercial 15% solution by weight of $\text{C}_2\text{H}_5\text{ONO}$ in ethanol (Aldrich Chemical Co.), and both nitrites were stored at 77 K under vacuum.

Results

Kinetic Studies. The data obtained from a series of irradiated $\text{CH}_3\text{ONO}\text{--NO}\text{--}2\text{-pentanone}\text{--}2\text{-heptanone}\text{--cyclohexane}\text{--air}$ mixtures are plotted in accordance with eq 1 in Figure 1. Good straight line plots are observed, and the rate constant ratios k_1/k_2 obtained from these plots by least-squares analyses are given in Table 1. These rate constant ratios k_1/k_2 are placed on an absolute basis by use of a rate constant k_2 for the reaction of the OH radical with cyclohexane of $k_2 = 7.21 \times 10^{-12}\text{ cm}^3\text{ molecule}^{-1}\text{ s}^{-1}$ at 298 K (14), and the resulting rate constants k_1 are given in Table 1.

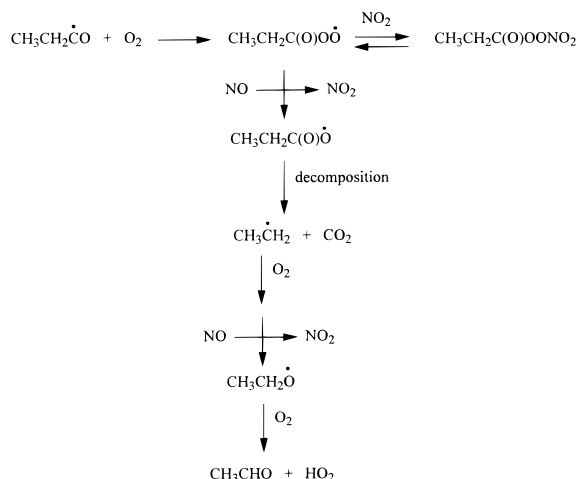
Product Studies. **Teflon Chamber with Analysis by GC-FID.** GC-FID and GC–MS analyses of irradiated $\text{CH}_3\text{ONO}\text{--NO}\text{--}2\text{-pentanone}$ (or 2-heptanone)–air mixtures showed the formation of acetaldehyde, propanal, and 2,4-pentanedione $[\text{CH}_3\text{C}(\text{O})\text{CH}_2\text{C}(\text{O})\text{CH}_3]$ from 2-pentanone and the formation of acetaldehyde, propanal, butanal, and pentanal from 2-heptanone. These products also react with the OH radical,

TABLE 1. Rate Constant Ratios k_1/k_2 and Rate Constants k_1 for the Gas-Phase Reactions of the OH Radical with 2-Pentanone and 2-Heptanone at Room Temperature

ketone	k_1/k_2^a	$10^{12} \times k_1$ ($\text{cm}^3 \text{ molecule}^{-1} \text{ s}^{-1}$)		temp (K)	reference
		this work ^b	literature		
2-pentanone	0.633 ± 0.041	4.56 ± 0.30	4.53 ± 0.14^c	299 ± 2	Atkinson et al. (4)
			4.00 ± 0.29	296	Wallington and Kurylo (5)
			4.88 ± 0.25^c	296 ± 2	Atkinson and Aschmann (6)
2-heptanone	1.62 ± 0.14	11.7 ± 1.1	8.67 ± 0.84	296	Wallington and Kurylo (5)

^a Indicated errors are two least-squares standard deviations. ^b At 298 ± 2 K. Placed on an absolute basis using a rate constant of $k_2(\text{cyclohexane}) = 7.21 \times 10^{-12} \text{ cm}^3 \text{ molecule}^{-1} \text{ s}^{-1}$ at 298 K (14). Indicated errors are two least-squares standard deviations and do not take into account the uncertainties associated with the rate constant k_2 . ^c Relative rate study with cyclohexane as the reference organic. Placed on an absolute basis using a rate constant of $k_2 = 2.88 \times 10^{-17} T^2 e^{309/T} \text{ cm}^3 \text{ molecule}^{-1} \text{ s}^{-1}$ (14).

SCHEME 1



and their secondary reactions were taken into account as described previously (15) with rate constants for the reactions of the OH radical (in units of $10^{-12} \text{ cm}^3 \text{ molecule}^{-1} \text{ s}^{-1}$) as follows: 2-pentanone, 4.66 (this and previous work from this laboratory, see below); 2-heptanone, 11.7 (this work, see below); acetaldehyde, 15.8 (1); propanal, 19.6 (1); butanal, 23.5 (1); pentanal, 28.5 (9); and 2,4-pentanedione, 1.15 (16). The multiplicative factors F to take into account the secondary reactions of OH radicals with the carbonyl products increase with the rate constant ratio $k(\text{OH} + \text{product})/k(\text{OH} + \text{ketone})$ and with the extent of reaction (15). The maximum values of F were as follows: acetaldehyde, 1.92 (2-pentanone reactions) and 1.84 (2-heptanone reactions); propanal, 2.20 (2-pentanone reactions) and 2.09 (2-heptanone reactions); butanal, 2.37 (2-heptanone reactions); pentanal, 2.77 (2-heptanone reactions); and 2,4-pentanedione, 1.06 (2-pentanone reactions).

Secondary reactions of OH radicals with the aldehyde products can lead to the formation of the corresponding aldehyde with one less carbon atom (1, 2); for example, butanal from pentanal, propanal from butanal, and acetaldehyde from propanal by reactions such as those shown in Scheme 1. Hence the observed concentrations of butanal, propanal, and acetaldehyde (and especially of acetaldehyde and propanal) may be influenced by secondary formation from higher aldehydes. Plots of the amounts of acetaldehyde, propanal, and 2,4-pentanedione formed (corrected for reactions of the products with the OH radical) against the amounts of 2-pentanone reacted were good straight lines and the product formation yields obtained by least-squares analyses are given in Table 2. Plots of the amounts of aldehydes formed against the amounts of 2-heptanone reacted, shown in Figure 2, are good straight lines for pentanal (as expected, since pentanal is not expected to be a secondary product) and butanal, but there is curvature in the propanal and acetal-

TABLE 2. Products Observed and Their Formation Yields from the Reactions of the OH Radical with 2-Pentanone and 2-Heptanone in the Presence of NO

product	formation yield	
	GC-FID ^a	FT-IR ^b
2-Pentanone Reaction		
formaldehyde		1.03 ± 0.10
acetaldehyde	0.51 ± 0.11	
propanal	0.19 ± 0.03	
2,4-pentanedione	0.12 ± 0.03	
organic nitrates		0.12 ± 0.04
2-Heptanone Reaction		
formaldehyde		0.38 ± 0.08
acetaldehyde	0.15 ± 0.03 (0.05) ^c	
propanal	0.10 ± 0.02 (0.05) ^c	
butanal	0.07 ± 0.01	
pentanal	0.09 ± 0.01	
organic nitrates		0.18 ± 0.05

^a Indicated errors are two least-squares standard deviations combined with estimated uncertainties in the GC-FID response factors for the carbonyls of $\pm 5\%$ each. ^b Estimated overall uncertainties. ^c Values in parentheses are the initial formation yields obtained using second-order regression analyses (see text and Figure 2).

dehyde plots, with higher formation yields at larger extents of reaction (Figure 2). Analyses of the data using second-order regressions results in the fits shown in Figure 2. The butanal and pentanal concentrations (corrected for secondary reaction with the OH radical) are clearly fit well by first-order regressions (the initial slopes of the second-order fits are indistinguishable from the slopes of the linear least-squares analyses and the coefficients for the $([\text{2-heptanone}] \text{ reacted})^2$ term are close to zero), while the data for acetaldehyde and propanal are better fit by second-order regressions. The initial slopes of the second-order regressions for acetaldehyde and propanal are also given in Table 2 together with the least-squares slopes of the first-order regressions.

Teflon Chamber with Analyses by API-MS. API-MS/MS daughter ion and parent ion spectra were obtained for ion peaks observed in the API-MS analyses of irradiated $\text{CH}_3\text{ONO-NO-2-pentanone-air}$ and $\text{CH}_3\text{ONO-NO-2-heptanone-air}$ mixtures. Product ion peaks were identified based on the observation of homo- or heterodimer ions (for example, $[(M_{P1})_2 + H]^+$, $[(M_{P2})_2 + H]^+$, and $[M_{P1} + M_{P2} + H]^+$, where P1 and P2 are products or the 2-pentanone and 2-heptanone reactants) in the API-MS/MS parent ion spectra and consistency of the API-MS/MS daughter ion spectrum of a homo- or heterodimer ion with the parent ion spectra of the various $[M_p + H]^+$ ion peaks, as described in detail previously (12). Water cluster ion peaks of the product ions, $[M + H + H_2O]^+$, were also occasionally observed.

Products of molecular weight 100 (attributed to 2,4-pentanedione) and 147 were observed from the 2-pentanone reaction, and products of molecular weight 128, 144, and

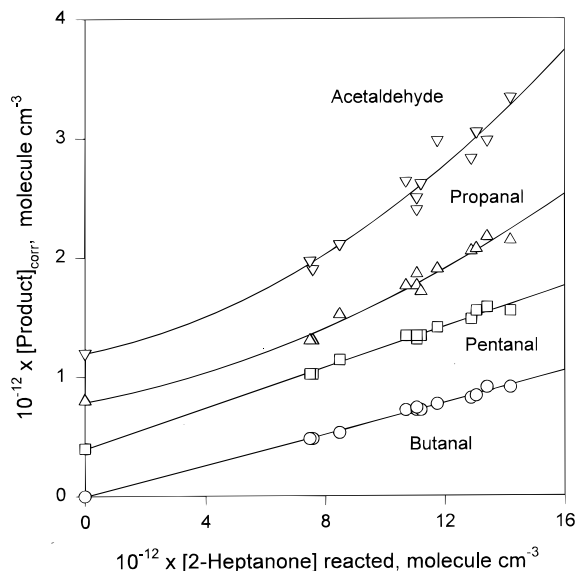


FIGURE 2. Plots of the amounts of acetaldehyde, propanal, butanal, and pentanal formed, corrected for reaction with the OH radical, against the amounts of 2-heptanone reacted with the OH radical in the presence of NO using second-order regression analyses (see text). Analyses by GC-FID. The concentrations of pentanal, propanal, and acetaldehyde have been displaced vertically by 4×10^{11} , 8×10^{11} , and 1.2×10^{12} molecule cm^{-3} , respectively, for clarity.

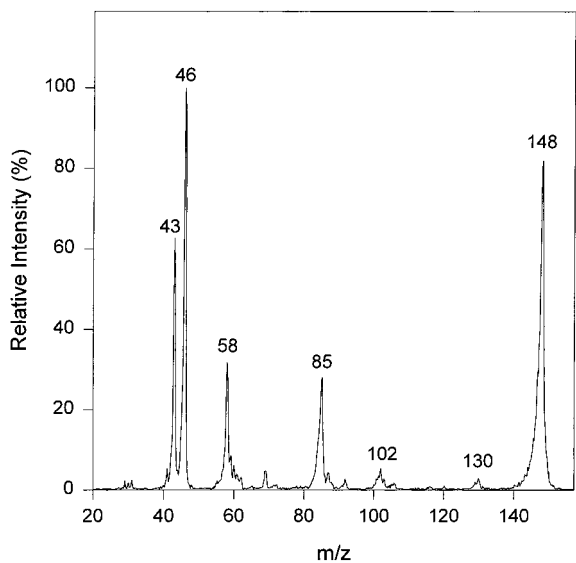


FIGURE 3. API-MS/MS CAD "daughter ion" spectrum of the 148 u ion peak observed in the API-MS analyses of irradiated $\text{CH}_3\text{ONO}-\text{NO}-2$ -pentanone-air mixtures. The 85 u ion peak is attributed to a loss of HNO_3 , and the 46 u fragment ion is attributed to NO_2^+ .

175 were observed from the 2-heptanone reaction. Figures 3 and 4 show the API-MS/MS CAD daughter ion spectra of the 148 and 176 u $[\text{M} + \text{H}]^+$ ions observed in the 2-pentanone and 2-heptanone reactions, respectively, with these spectra indicating that these molecular weight 147 and 175 products are (as expected from their odd molecular weights) organic nitrates (i.e., from the observations of a loss of HNO_3 and the presence of a 46 u NO_2^+ fragment ion). The possible identities of the molecular weight 128 and 144 products from the 2-heptanone reaction are dealt with in the Discussion section below.

Evacuable Chamber Experiments with FT-IR Analysis. Analyses of reactants and products during irradiated methyl (and ethyl) nitrite-NO-2-pentanone (or 2-heptanone)-air mixtures were carried out by in situ FT-IR absorption

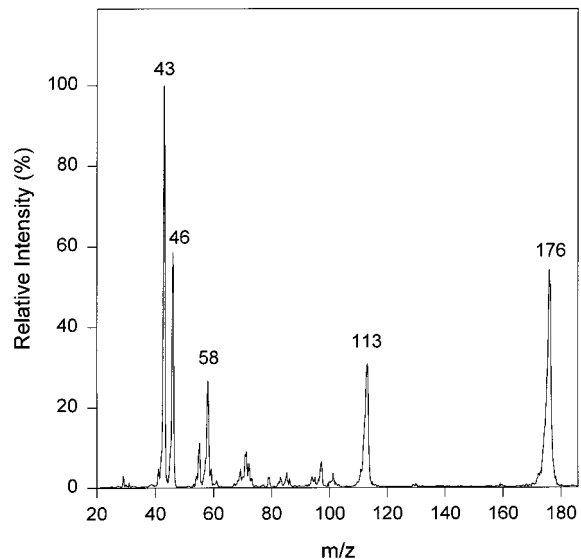


FIGURE 4. API-MS/MS CAD "daughter ion" spectrum of the 176 u ion peak observed in the API-MS analyses of irradiated $\text{CH}_3\text{ONO}-\text{NO}-2$ -heptanone-air mixtures. The 113 u ion peak is attributed to a loss of HNO_3 , and the 46 u fragment ion is attributed to NO_2^+ .

spectroscopy. Identification and quantification of carbonyl group-containing species was rendered difficult because products containing carbonyl groups absorb in the same $\sim 1740 \text{ cm}^{-1}$ region as do 2-pentanone and 2-heptanone. Indeed, GC-FID analyses (with sampling modifications to allow for the higher concentrations involved) were required to aid in determining the amounts of 2-pentanone and 2-heptanone reacted during the experiments, and analyses of carbonyl products other than HCHO (for example, those observed by GC-MS and API-MS analyses and shown in Table 2) by FT-IR spectroscopy was not possible.

Figure 5A shows a vapor-phase infrared spectrum of 2-pentanone. Figure 5B is the product spectrum obtained from a $\text{CH}_3\text{ONO}-\text{NO}-2$ -pentanone-air mixture after 32 min of irradiation that resulted in 14.3% consumption of the initial 2.46×10^{14} molecule cm^{-3} of 2-pentanone. In Figure 5B, the absorptions by the remaining reactants (the 2-pentanone concentrations were determined in part by concurrent GC analyses) and by the products attributed to the photooxidation of methyl nitrite in the presence of NO (HCHO , CH_3ONO_2 , HCOOH , NO_2 , HONO , and HNO_3) have been subtracted from the plot. Figure 5C is the residual spectrum after subtraction from Figure 5B of the absorptions by peroxyacyl nitrates, specifically 1.4×10^{13} molecule cm^{-3} of peroxyacetyl nitrate [$\text{CH}_3\text{C}(\text{O})\text{OONO}_2$; PAN] (Figure 5D) and 4.3×10^{12} molecule cm^{-3} of peroxypropionyl nitrate [$\text{CH}_3\text{-CH}_2\text{C}(\text{O})\text{OONO}_2$; PPN] (Figure 5E). PAN and PPN are secondary products arising from the expected products acetaldehyde and propanal (1, 2), and their apparent yields increased with the extent of reaction. In Figure 5C, and as noted above, the acetaldehyde and propanal absorptions could not be accurately distinguished from each other and from other possible carbonyl products.

In Figure 5C and in a similar product spectrum obtained for the case of 2-heptanone, distinct absorption bands near 856, 1285, and 1655 cm^{-1} indicate the formation of organic nitrates (RONO_2). The specific RONO_2 product(s) formed could not be identified. However, an estimate of the molar RONO_2 concentration was made from the integrated intensity of the $\sim 1655 \text{ cm}^{-1}$ absorption band (assigned to the asymmetric NO_2 stretch and which is distinct from that of ROONO_2 species) and the average integrated absorption coefficient of the corresponding bands of other organic nitrates. Thus, measurements in this laboratory on the corresponding bands

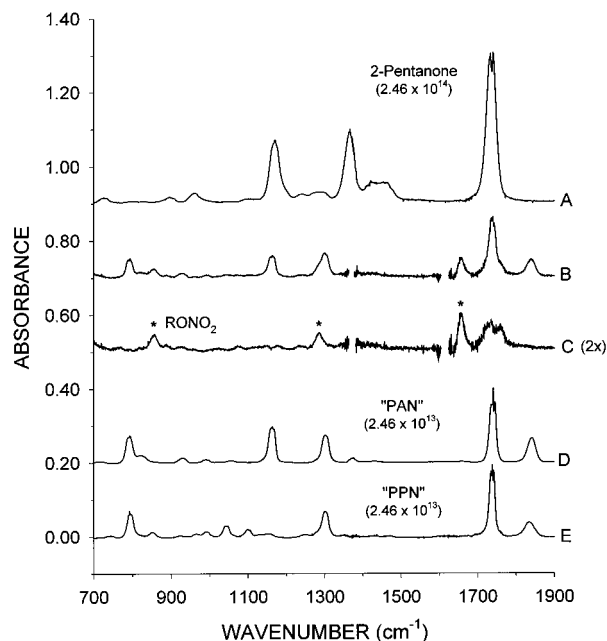


FIGURE 5. Infrared spectra from a $\text{CH}_3\text{ONO}-\text{NO}-2$ -pentanone-air irradiation. (A) Initial 2-pentanone. (B) Products (except HCHO) corresponding to 14.3% consumption of the initial 2-pentanone. (C) From panel B with absorptions by peroxyacetyl nitrate (PAN) and peroxypropionyl nitrate (PPN) subtracted. (D) PAN reference spectrum. (E) PPN reference spectrum. Numbers in parentheses are the concentrations in molecule cm^{-3} . Gaps in the traces of panels B and C correspond to strong absorptions by NO_2 formed and to accumulated NO_3^- ions on the KBr windows.

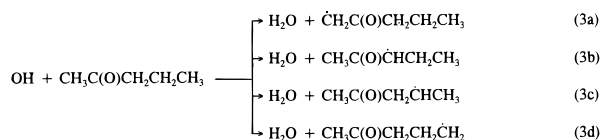
of methyl nitrate, ethyl nitrate, 1-propyl nitrate, and peroxyacetyl nitrate (PAN) showed an average integrated absorption coefficient (base 10) of $(2.5 \pm 0.2) \times 10^{-17} \text{ cm molecule}^{-1}$ (10). Using this value, the average RONO_2 yields obtained from 2-pentanone and 2-heptanone are given in Table 2, where the cited estimated overall uncertainties include the uncertainties associated with the absorption coefficient used.

The yields of HCHO were determined by FT-IR spectroscopy from irradiated $\text{C}_2\text{H}_5\text{ONO}-\text{NO}-2$ -pentanone (or 2-heptanone)-air mixtures, with subtraction of the parent ketone absorptions again being indexed to the GC-FID analyses. The product spectra obtained by subtraction of absorptions by the remaining reactants and byproducts attributed to ethyl nitrite photolysis in the presence of NO (CH_3CHO , $\text{C}_2\text{H}_5\text{ONO}$, NO_2 , HONO, and HNO_3) were similar to those from experiments that employed methyl nitrite, except for larger quantities of PAN formed as a secondary product of ethyl nitrite. The exact subtraction of absorptions by CH_3CHO and other carbonyl products was not necessary since the analysis of HCHO was based on its sharp Q-branch feature at 1745 cm^{-1} , which is readily distinguished from the other, much broader $\text{C}=\text{O}$ stretch absorption bands. HCHO measurements were obtained within a 12-min total irradiation period and 12.0% consumption of 2-pentanone and within a 9-min total irradiation period and 15.2% consumption of 2-heptanone, with an initial concentration of $2.46 \times 10^{14} \text{ molecule cm}^{-3}$ for each reactant ketone. The measured HCHO concentrations were corrected for secondary reaction with the OH radical using an OH radical reaction rate constant of $9.37 \times 10^{-12} \text{ cm}^3 \text{ molecule}^{-1} \text{ s}^{-1}$ (1), with the multiplicative correction factors to take into account secondary reactions being <1.17 for the 2-pentanone reactions and <1.11 for the 2-heptanone reactions. The formation yields of HCHO obtained from least-squares analyses of the data are given in Table 2.

Discussion

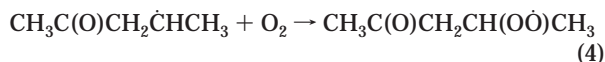
2-Pentanone Reaction. As shown in Table 1, our present rate constant for the reaction of the OH radical with 2-pentanone is in excellent agreement (to within 7%) with those previously measured in this laboratory (4, 6) and is in good agreement with, being 14% higher than, the absolute rate constant of Wallington and Kurylo (5). We have used an average of the three relative rate measurements of the rate constant of $k_1(2\text{-pentanone}) = 4.66 \times 10^{-12} \text{ cm}^3 \text{ molecule}^{-1} \text{ s}^{-1}$ for the purposes of correcting for secondary reactions of the products observed (see above).

The OH radical reaction with 2-pentanone can proceed by four pathways, all involving H-atom abstraction from the C-H bonds (1).

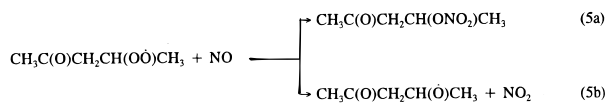


The empirical estimation method of Kwok and Atkinson (17) predicts the total OH radical reaction rate constant for 2-pentanone to within 5% of the measured value, and further predicts that reaction pathways 3a-d account for 2%, 18%, 76%, and 3.5%, respectively, of the total reaction.

In the troposphere, the alkyl radicals formed in reactions 3a-d react solely with O_2 to form the corresponding peroxy radicals (1, 14), as shown for the $\text{CH}_3\text{C}(\text{O})\text{CH}_2\dot{\text{C}}\text{HCH}_3$ radical:



Under the conditions employed in our experiments, the organic peroxy radicals then react with NO to form the corresponding alkoxy radical plus NO_2 or the organic nitrate (RONO_2) (1, 2).

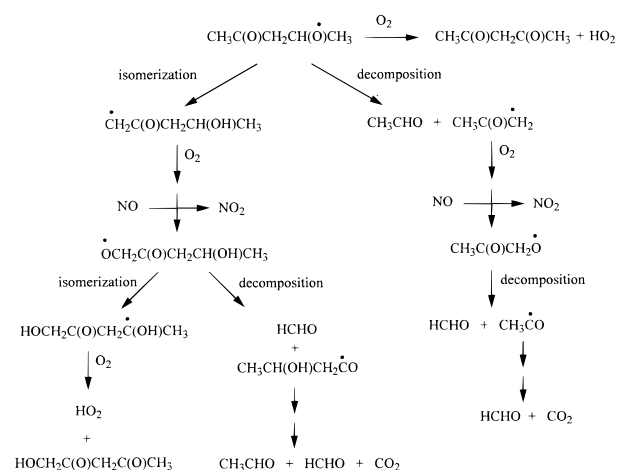


The organic nitrates formed from the reactions of the peroxy radicals with NO [$\text{CH}_3\text{C}(\text{O})\text{CH}_2\text{CH}_2\text{CH}_2\text{ONO}_2$, $\text{CH}_3\text{C}(\text{O})\text{CH}_2\text{CH}(\text{ONO}_2)\text{CH}_3$, $\text{CH}_3\text{C}(\text{O})\text{CH}(\text{ONO}_2)\text{CH}_2\text{CH}_3$, and $\text{O}_2\text{NOCH}_2\text{C}(\text{O})\text{CH}_2\text{CH}_2\text{CH}_3$] have a molecular weight of 147, and their formation is consistent with our API-MS and API-MS/MS observations of a product(s) of molecular weight 147 (Figure 3) and with the in situ FT-IR analyses discussed above.

The alkoxy radicals then react via a number of pathways, involving decomposition by C-C bond scission, isomerization via a six-membered transition state, and reaction with O_2 (1, 14, 18) [noting that not all of these three reaction pathways are possible for all four of the alkoxy radicals initially formed from 2-pentanone]. Scheme 2 shows the possible reactions of the $\text{CH}_3\text{C}(\text{O})\text{CH}_2\text{CH}(\text{O})\text{CH}_3$ radical leading to first-generation products [the detailed reactions of $\dot{\text{C}}\text{H}_3$ and acyl ($\text{RC}(\text{O})\text{O}$) radicals are not shown for clarity, rather the known products (1, 2) are shown].

$\dot{\text{O}}\text{CH}_2\text{C}(\text{O})\text{CH}_2\text{CH}_2\text{CH}_3$ Radical. This alkoxy radical can decompose, isomerize, or react with O_2 . On the basis of the reactions of the $\text{CH}_3\text{C}(\text{O})\text{CH}_2\dot{\text{O}}$ and $\text{CH}_3\text{C}(\text{O})\text{CH}(\dot{\text{O}})\text{CH}_3$ radicals of similar structure formed from acetone and 2-butanone, respectively, for which the decomposition reactions dominate over reaction with O_2 (19, 20), the O_2 reaction is anticipated to be of negligible importance. The $\dot{\text{O}}\text{CH}_2\text{C}(\text{O})\text{CH}_2\text{CH}_2\text{CH}_3$ radical can also isomerize, but it is

SCHEME 2

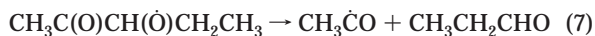


not known, a priori, how important this pathway is. The decomposition reaction



leads to the formation of the acyl radical $\text{CH}_3\text{CH}_2\text{CH}_2\dot{\text{C}}\text{O}$, which will react in the atmosphere (via the intermediary of the acyl peroxy radical $\text{CH}_3\text{CH}_2\text{CH}_2\text{C}(\text{O})\text{OO}\dot{\text{O}}$) to form the 1-propyl radical, which will react to form propanal [plus a small amount of 1-propyl nitrate] (1, 14).

$\text{CH}_3\text{C}(\text{O})\text{CH}(\dot{\text{O}})\text{CH}_2\text{CH}_3$ Radical. This alkoxy radical can decompose or react with O_2 . On the basis of the reactions of the analogous $\text{CH}_3\text{C}(\text{O})\text{CH}_2\dot{\text{O}}$ and $\text{CH}_3\text{C}(\text{O})\text{CH}(\dot{\text{O}})\text{CH}_3$ radicals (19, 20), the decomposition reaction is anticipated to totally dominate under our conditions:

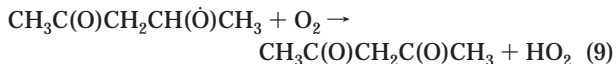


The alternative decomposition pathway to $\text{CH}_3\text{C}(\text{O})\text{CHO} + \text{CH}_3\dot{\text{C}}\text{H}_2$ is thermochemically less favorable by $\sim 11 \text{ kcal mol}^{-1}$ (21) and is therefore expected to be of minor or negligible importance. The acetyl radical, $\text{CH}_3\dot{\text{C}}\text{O}$, will react to form HCHO plus CO_2 (1, 2).

$\text{CH}_3\text{C}(\text{O})\text{CH}_2\text{CH}(\dot{\text{O}})\text{CH}_3$ Radical. As shown in Scheme 2, this alkoxy radical can decompose, isomerize, or react with O_2 . For the analogous radical $\text{CH}_3\text{C}(\text{O})\text{CH}_2\text{C}(\dot{\text{O}})(\text{CH}_3)_2$ formed from 4-methyl-2-pentanone, Atkinson and Aschmann (22) showed that isomerization did not compete with decomposition, with the decomposition rate of the $\text{CH}_3\text{C}(\text{O})\text{CH}_2\text{C}(\dot{\text{O}})(\text{CH}_3)_2$ radical being estimated (14, 18) to be $\sim 4 \times 10^5 \text{ s}^{-1}$ at 298 K. Hence, it is possible that the dominant reactions of the $\text{CH}_3\text{C}(\text{O})\text{CH}_2\text{CH}(\dot{\text{O}})\text{CH}_3$ radical are by decomposition and/or reaction with O_2 . The decomposition pathway

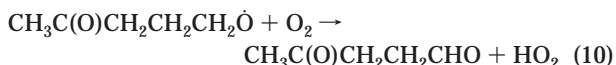
$\text{CH}_3\text{C}(\text{O})\text{CH}_2\text{CH}(\dot{\text{O}})\text{CH}_3 \rightarrow \text{CH}_3\text{CHO} + \text{CH}_3\text{C}(\text{O})\dot{\text{C}}\text{H}_2 \quad (8)$

followed by reactions of the $\text{CH}_3\text{C}(\text{O})\dot{\text{C}}\text{H}_2$ radical under tropospheric conditions results in the formation of CH_3CHO , 2HCHO , and CO_2 (1, 2), while the O_2 reaction



leads to the observed product 2,4-pentanedione.

$\text{CH}_3\text{C}(\text{O})\text{CH}_2\text{CH}_2\text{CH}_2\dot{\text{O}}$ Radical. This alkoxy radical can decompose or react with O_2 (but not isomerize through a six-membered transition state). The estimation method of Atkinson (14, 18) predicts that reaction with O_2 will dominate at room temperature and atmospheric pressure of air:



leading to the formation of the molecular weight 100 keto-aldehyde $\text{CH}_3\text{C}(\text{O})\text{CH}_2\text{CH}_2\text{CHO}$.

Table 3 gives the potential products arising from the four initially formed peroxy radicals, together with an a priori estimate of the relative importance of the particular pathways based on the discussion given in Atkinson and Aschmann (22) and Atkinson (14, 18). Given the expected low formation yields of $\dot{\text{C}}\text{H}_2\text{C}(\text{O})\text{CH}_2\text{CH}_2\text{CH}_3$ and $\text{CH}_3\text{C}(\text{O})\text{CH}_2\text{CH}_2\text{CH}_2\dot{\text{O}}$ radicals, then the expected major products from the OH radical reaction with 2-pentanone in the presence of NO are the molecular weight 147 $\text{C}_5\text{H}_9\text{O}(\text{ONO}_2)$ nitrates formed from the $\text{RO}_2 + \text{NO}$ reactions, $\text{CH}_3\text{C}(\text{O})\text{CH}_2\text{C}(\text{O})\text{CH}_3$, $\text{CH}_3\text{CHO} + 2\text{HCHO}$ and/or isomerization products from the $\text{CH}_3\text{C}(\text{O})\text{CH}_2\text{CH}(\dot{\text{O}})\text{CH}_3$ radical, and $\text{CH}_3\text{CH}_2\text{CHO} + \text{HCHO}$ from the $\text{CH}_3\text{C}(\text{O})\text{CH}(\dot{\text{O}})\text{CH}_2\text{CH}_3$ radical. Our experimental data are in agreement with these expectations, with $19 \pm 3\%$ propanal (plus coproduct HCHO) arising from the $\text{CH}_3\text{C}(\text{O})\text{CH}(\dot{\text{O}})\text{CH}_2\text{CH}_3$ radical and $51 \pm 11\%$ acetaldehyde (plus coproduct HCHO with twice the acetaldehyde yield) and $12 \pm 3\%$ 2,4-pentanedione arising from the $\text{CH}_3\text{C}(\text{O})\text{CH}_2\text{CH}(\dot{\text{O}})\text{CH}_3$ radical. Our observed HCHO yield of $103 \pm 10\%$ agrees reasonably well with that of $121 \pm 23\%$ expected from HCHO being a coproduct to the acetaldehyde and propanal products. Our observed products account for $94 \pm 13\%$ of the total reaction pathways and the amounts of products arising from the

TABLE 3. Potential First-Generation Products Arising from the Initially Formed Alkoxy Radicals Formed in the Reaction of the OH Radical with 2-Pentanone

R $\dot{\text{O}}$ radical	reaction pathway	product
$\dot{\text{O}}\text{CH}_2\text{C}(\text{O})\text{CH}_2\text{CH}_2\text{CH}_3$ (2%)	O_2 reaction ^a decomposition isomerization	$\text{CH}_3\text{CH}_2\text{CH}_2\text{C}(\text{O})\text{CHO}$ $\text{HCHO} + \text{CH}_3\text{CH}_2\text{CHO}$ $\text{HOCH}_2\text{C}(\text{O})\text{CH}_2\text{C}(\text{O})\text{CH}_3$ or $\text{CH}_3\text{CHO} + 2\text{HCHO}$ or $\text{CH}_3\text{CH}(\text{OH})\text{CH}_2\text{C}(\text{O})\text{CHO}$
$\text{CH}_3\text{C}(\text{O})\text{CH}(\dot{\text{O}})\text{CH}_2\text{CH}_3$ (18%)	O_2 reaction ^a decomposition ^b decomposition	$\text{CH}_3\text{C}(\text{O})\text{C}(\text{O})\text{CH}_2\text{CH}_3$ $\text{CH}_3\text{C}(\text{O})\text{CHO} + \text{CH}_3\text{CHO}$ $\text{CH}_3\text{CH}_2\text{CHO} + \text{HCHO}$
$\text{CH}_3\text{C}(\text{O})\text{CH}_2\text{CH}(\dot{\text{O}})\text{CH}_3$ (76%)	O_2 reaction decomposition isomerization	$\text{CH}_3\text{C}(\text{O})\text{CH}_2\text{C}(\text{O})\text{CH}_3$ $\text{CH}_3\text{CHO} + 2\text{HCHO}$ $\text{HOCH}_2\text{C}(\text{O})\text{CH}_2\text{C}(\text{O})\text{CH}_3$ or $\text{CH}_3\text{CHO} + 2\text{HCHO}$
$\text{CH}_3\text{C}(\text{O})\text{CH}_2\text{CH}_2\text{CH}_2\dot{\text{O}}$ (3.5%)	O_2 reaction decomposition ^a decomposition ^a	$\text{CH}_3\text{C}(\text{O})\text{CH}_2\text{CH}_2\text{CHO}$ $\text{HCHO} + \text{CH}_3\text{C}(\text{O})\text{CH}_2\text{CHO}$ 4HCHO

^a Reaction pathways expected to be of minor importance (1, 14, 18). ^b Expected to be minor relative to the other decomposition pathway.

TABLE 4. Potential First-Generation Products Arising from the Initially Formed Alkoxy Radicals from the Reaction of the OH Radical with 2-Heptanone

R \dot{O} radical	reaction pathway	product
$\dot{O}CH_2C(O)CH_2CH_2CH_2CH_2CH_3$ (1%)	O ₂ reaction ^a decomposition isomerization isomerization	CH ₃ CH ₂ CH ₂ CH ₂ CH ₂ C(O)CHO HCHO + CH ₃ CH ₂ CH ₂ CH ₂ CHO HOCH ₂ C(O)CH ₂ C(O)CH ₂ CH ₂ CH ₂ OH CH ₃ CH ₂ CH ₂ CH(OH)CH ₂ C(O)CHO
CH ₃ C(O)CH(\dot{O})CH ₂ CH ₂ CH ₂ CH ₃ (11%)	O ₂ reaction ^a decomposition ^b	CH ₃ C(O)C(O)CH ₂ CH ₂ CH ₂ CH ₃ CH ₃ C(O)CHO + 0.23CH ₃ CH ₂ CH ₂ CHO + 0.77HOCH ₂ CH ₂ CH ₂ CHO
CH ₃ C(O)CH ₂ CH(\dot{O})CH ₂ CH ₂ CH ₃ (55%)	decomposition isomerization O ₂ reaction decomposition decomposition isomerization	CH ₃ CH ₂ CH ₂ CH ₂ CHO + HCHO CH ₃ C(O)C(O)CH ₂ CH ₂ CH(OH)CH ₃ CH ₃ C(O)CH ₂ C(O)CH ₂ CH ₂ CH ₃ CH ₃ CH ₂ CH ₂ CHO + 2HCHO CH ₃ C(O)CH ₂ CHO + CH ₃ CH ₂ CHO
CH ₃ C(O)CH ₂ CH ₂ CH(\dot{O})CH ₂ CH ₃ (17%)	O ₂ reaction decomposition decomposition decomposition	CH ₃ C(O)CH ₂ C(O)CH ₂ CH ₂ CH ₂ OH CH ₃ C(O)CH ₂ CH ₂ C(O)CH ₂ CH ₃ CH ₃ CHO + CH ₃ C(O)CH ₂ CH ₂ CHO CH ₃ CH ₂ CHO + CH ₃ C(O)CH ₂ CHO
CH ₃ C(O)CH ₂ CH ₂ CH ₂ CH(\dot{O})CH ₃ (14%)	O ₂ reaction decomposition isomerization isomerization	CH ₃ C(O)CH ₂ CH ₂ CH ₂ C(O)CH ₃ CH ₃ CHO + CH ₃ C(O)CH ₂ CH ₂ CHO CH ₃ C(O)CH(OH)CH ₂ CH ₂ C(O)CH ₃ HCHO + CH ₃ CH(OH)CH ₂ CH ₂ CHO
CH ₃ C(O)CH ₂ CH ₂ CH ₂ CH ₂ CH \dot{O} (2%)	O ₂ reaction decomposition ^a isomerization	CH ₃ C(O)CH ₂ CH ₂ CH ₂ CH ₂ CHO HCHO + CH ₃ C(O)CH ₂ CH ₂ CH ₂ CHO CH ₃ C(O)CH ₂ CH(OH)CH ₂ CH ₂ CHO

^a Reaction pathways expected to be of minor importance. ^b This pathway expected to be less important than the other decomposition pathway.

CH₃C(O)CH(\dot{O})CH₂CH₃ and CH₃C(O)CH₂CH(\dot{O})CH₃ radicals (19 ± 3% and 63 ± 12%, respectively) are similar to the predicted percentages of the alkoxy radicals formed [18% and 76% formation of their precursor peroxy radicals (17), with the occurrence of organic nitrate formation from the R \dot{O}_2 + NO reactions leading to slightly lower formation yields of the alkoxy radicals]. It is entirely possible that the products formed from the CH₃C(O)CH₂CH₂CH \dot{O} radical in low overall yield and any isomerization products of the CH₃C(O)CH₂CH(\dot{O})CH₃ radical were not identified and quantified and account in part for the ≤19% products not presently accounted for (noting that within the uncertainties our product yields do account for 100% of the reaction pathways).

2-Heptanone Reaction. As shown in Table 1, our present rate constant for the reaction of the OH radical with 2-heptanone is 35% higher than the absolute rate constant determined by Wallington and Kurylo (5). As noted in the Introduction, there are also discrepancies between the absolute rate study of Wallington and Kurylo (5) and our previous relative rate measurements (4, 6) for the reactions of the OH radical with 2- and 3-pentanone and 2-hexanone. The absolute rate method used by Wallington and Kurylo (5) required that the ketone concentrations in the reaction vessel be known, and these were calculated from the flows of the various reactant gas streams entering the reaction vessel. It is possible that in the Wallington and Kurylo (5) study the larger ketones were subject to wall losses, thereby resulting in erroneously low measured rate constants.

As for 2-pentanone, the OH radical reaction with 2-heptanone proceeds by H-atom abstraction from the various C–H bonds. The resulting alkyl-type radicals will add O₂ to form organic peroxy (R \dot{O}_2) radicals. These R \dot{O}_2 radicals then react with NO to form either the molecular weight 175 organic nitrates observed by API-MS and API-MS/MS analyses (Figure 4) and consistent with our in situ FT-IR analyses or the corresponding alkoxy radical plus NO₂ as shown in reactions 5a and 5b above for the 2-pentanone reaction. The alkoxy radicals formed, the estimated percent of the precursor peroxy radicals formed (17), and the potential first-generation products formed from their subsequent reactions are given in Table 4 together with an a priori assessment of the relative importance of the particular reaction pathways based on the

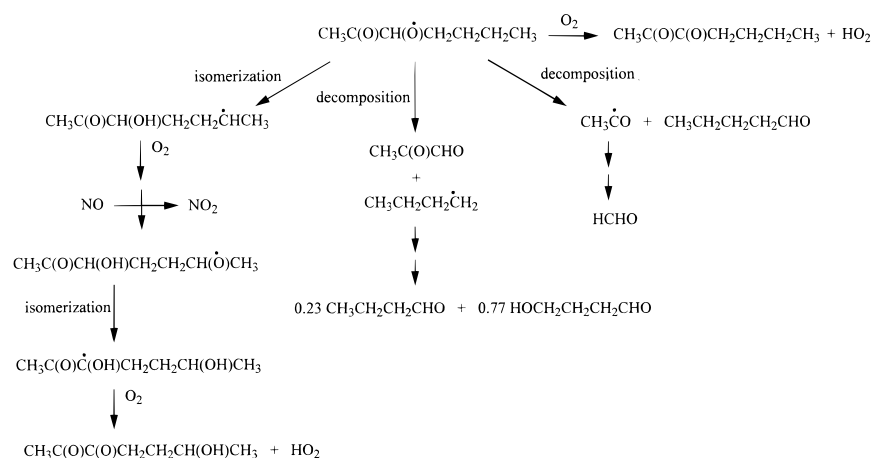
discussion given in Atkinson and Aschmann (22) and Atkinson (1, 14, 18). As an example of these reaction pathways, Scheme 3 shows the possible reaction pathways for the alkoxy radical CH₃C(O)CH(\dot{O})CH₂CH₂CH₂CH₃ [the reactions of the CH₃CH₂CH₂CH \dot{O} and CH₃CO are not shown in detail, because under atmospheric conditions the CH₃CH₂CH₂CH \dot{O} radical is known to form CH₃CH₂CH₂CHO (23%) plus HOCH₂CH₂CH₂CHO (77%) and the CH₃CO radical leads to the formation of HCHO (1, 2, 14, 18)]. Our conclusions concerning the reactions of the four major initially formed alkoxy radicals are briefly discussed below.

CH₃C(O)CH(\dot{O})CH₂CH₂CH₂CH₃ Radical. The only route to formation of pentanal is via decomposition of the CH₃C(O)CH(\dot{O})CH₂CH₂CH₂CH₃ radical (Table 4). Furthermore, the formation yield of pentanal (9 ± 1%) is similar to the calculated formation yield of the CH₃C(O)CH(\dot{O})CH₂CH₂CH₂CH₃ radical of ≤11% (17) [with the calculated yield of the CH₃C(O)CH(\dot{O})CH₂CH₂CH₂CH₃ radical depending on the amount of organic nitrate formed from the reaction of the CH₃C(O)CH(O \dot{O})CH₂CH₂CH₂CH₃ radical with NO]. Thus, the dominant reaction of the CH₃C(O)CH(\dot{O})CH₂CH₂CH₂CH₃ radical appears to be decomposition to form pentanal plus HCHO (Scheme 3).

CH₃C(O)CH₂CH(\dot{O})CH₂CH₂CH₃ Radical. The CH₃C(O)CH₂CH(\dot{O})CH₂CH₂CH₃ radical can decompose to form butanal plus two molecules of HCHO, decompose to form CH₃C(O)CH₂CHO plus propanal, react with O₂ to form the molecular weight 128 dicarbonyl CH₃C(O)CH₂C(O)CH₂CH₂CH₃, and isomerize to form mainly the molecular weight 144 hydroxydicarbonyl CH₃C(O)CH₂C(O)CH₂CH₂CH₂OH. Because the butanal formation yield from the 1-butoxy radical under atmospheric conditions is ~23% (1, 14) (Scheme 3 and Table 4), most, if not all, of the butanal observed must arise from decomposition of the CH₃C(O)CH₂CH(\dot{O})CH₂CH₂CH₃ radical with the remainder of the CH₃C(O)CH₂CH(\dot{O})CH₂CH₂CH₃ radical reacting with O₂ to form the molecular weight 128 dicarbonyl CH₃C(O)CH₂C(O)CH₂CH₂CH₃ and isomerizing to form mainly the molecular weight 144 hydroxydicarbonyl CH₃C(O)CH₂C(O)CH₂CH₂CH₂OH.

CH₃C(O)CH₂CH₂CH(\dot{O})CH₂CH₃ Radical. The CH₃C(O)CH₂CH₂CH(\dot{O})CH₂CH₃ radical can react with O₂ to form the molecular weight 128 dicarbonyl CH₃C(O)CH₂CH₂C(O)CH₂CH₃

SCHEME 3



CH₃, decompose to form acetaldehyde plus CH₃C(O)CH₂-CH₂CHO, or decompose to form propanal plus CH₃C(O)CH₂-CHO. On the basis of the reactions of alkoxy radicals (e.g., 2-butoxy and 3-pentoxo radicals) formed from the *n*-alkanes (14, 18), reaction with O₂ is expected to dominate over decomposition, and hence we anticipate the formation of the molecular weight 128 dicarbonyl CH₃C(O)CH₂CH₂C(O)-CH₂CH₃ from this radical.

CH₃C(O)CH₂CH₂CH₂CH(O)CH₃ Radical. The CH₃C(O)CH₂-CH₂CH₂CH(O)CH₃ radical can react with O₂ to form the molecular weight 128 dicarbonyl CH₃C(O)CH₂CH₂CH₂C(O)-CH₃, decompose to form acetaldehyde plus CH₃C(O)CH₂-CH₂CHO, and isomerize to form HCHO plus CH₃CH(OH)-CH₂CH₂CHO or the molecular weight 144 hydroxydicarbonyl CH₃C(O)CH(OH)CH₂CH₂C(O)CH₃. We expect that isomerization dominates (see also the discussion below).

As evident from Table 3, the reaction pathways leading to the formation of pentanal and butanal predict that the coproduct formaldehyde should have a yield of 23 ± 2% and suggest that the remaining 15 ± 9% of HCHO arises largely from the isomerization channel of the CH₃C(O)CH₂CH₂CH₂-CH(O)CH₃ radical (HCHO can also be formed as a result of secondary reactions of the other first-generation products such as acetaldehyde). Our data analysis therefore suggests that we have identified ~60% of the overall reaction pathways, with the formation of molecular weight 128 dicarbonyls such as CH₃C(O)CH₂C(O)CH₂CH₂CH₃, CH₃C(O)CH₂CH₂C(O)CH₂-CH₃, and CH₃C(O)CH₂CH₂CH₂C(O)CH₃ and molecular weight 144 hydroxydicarbonyls such as CH₃C(O)CH₂C(O)CH₂CH₂-CH₂OH accounting for the remaining ~40% of products that could not be quantified by gas chromatography or in situ FT-IR spectroscopy.

Tropospheric Lifetimes and Products. The reactions of the OH radical with 2-pentanone and 2-heptanone result in calculated lifetimes of these two ketones of 2.5 and 1.0 day, respectively, for a 24-h average OH radical concentration of 1.0 × 10⁶ molecule cm⁻³ (23, 24). Our product studies indicate that the reactions of 2-pentanone are relatively straightforward and involve reactions of the intermediate first-formed alkoxy radicals with O₂ and decomposition, while in the 2-heptanone system the first-formed intermediate alkoxy radicals also isomerize, with the isomerization reactions potentially dominating in some cases. Our product analyses

indicate that in general the reactions of the ketones are analogous to those of the alkanes, in that the intermediate alkoxy radicals can decompose, isomerize, and react with O₂. Furthermore, the occurrence of the alkoxy radical isomerization reaction (which proceeds through a six-membered transition state) becomes important for compounds with a ≥ 5-carbon chain (and was observed here for 2-heptanone).

Acknowledgments

The authors thank the Eastman Chemical Company for supporting this research, and Dr. David A. Morgott (Eastman Kodak Company) for helpful comments.

Literature Cited

- (1) Atkinson, R. *J. Phys. Chem. Ref. Data* **1994**, *Monograph 2*, 1–216.
- (2) Atkinson, R. *Atmos. Environ.*, in press.
- (3) Carter, W. P. L. *J. Air Waste Manage. Assoc.* **1994**, *44*, 881–899.
- (4) Atkinson, R.; Aschmann, S. M.; Carter, W. P. L.; Pitts, J. N., Jr. *Int. J. Chem. Kinet.* **1982**, *14*, 839–847.
- (5) Wallington, T. J.; Kurylo, M. J. *J. Phys. Chem.* **1987**, *91*, 5050–5054.
- (6) Atkinson, R.; Aschmann, S. M. *J. Phys. Chem.* **1988**, *92*, 4008.
- (7) Aschmann, S. M.; Atkinson, R. *Int. J. Chem. Kinet.* **1998**, *30*, 533–540.
- (8) Atkinson, R.; Carter, W. P. L.; Winer, A. M.; Pitts, J. N., Jr. *J. Air Pollut. Control Assoc.* **1981**, *31*, 1090–1092.
- (9) Atkinson, R. *J. Phys. Chem. Ref. Data* **1989**, *Monograph 1*, 1–246.
- (10) Tuazon, E. C.; Atkinson, R. *Int. J. Chem. Kinet.* **1990**, *22*, 1221–1236.
- (11) Atkinson, R.; Tuazon, E. C.; Aschmann, S. M. *Environ. Sci. Technol.* **1995**, *29*, 1674–1680.
- (12) Aschmann, S. M.; Chew, A. A.; Arey, J.; Atkinson, R. *J. Phys. Chem. A* **1997**, *101*, 8042–8048.
- (13) Taylor, W. D.; Allston, T. D.; Moscato, M. J.; Fazekas, G. B.; Kozlowski, R.; Takacs, G. A. *Int. J. Chem. Kinet.* **1980**, *12*, 231–240.
- (14) Atkinson, R. *J. Phys. Chem. Ref. Data* **1997**, *26*, 215–290.
- (15) Atkinson, R.; Aschmann, S. M.; Carter, W. P. L.; Winer, A. M.; Pitts, J. N., Jr. *J. Phys. Chem.* **1982**, *86*, 4563–4569.
- (16) Dagaut, P.; Wallington, T. J.; Liu, R.; Kurylo, M. J. *J. Phys. Chem.* **1988**, *92*, 4375–4377.
- (17) Kwok, E. S. C.; Atkinson, R. *Atmos. Environ.* **1995**, *29*, 1685–1695.
- (18) Atkinson, R. *Int. J. Chem. Kinet.* **1997**, *29*, 99–111.
- (19) Cox, R. A.; Patrick, K. F.; Chant, S. A. *Environ. Sci. Technol.* **1981**, *15*, 587–592.
- (20) Jenkin, M. E.; Cox, R. A.; Emrich, M.; Moortgat, G. K. *J. Chem. Soc., Faraday Trans.* **1993**, *89*, 2983–2991.
- (21) *Database 25: Structures and Properties Database and Estimation Program, Version 2.0*; Stein, S. E., Ed.; Chemical Kinetics and Thermodynamics Division, National Institute of Standards and Technology: Gaithersburg, MD, 1994.
- (22) Atkinson, R.; Aschmann, S. M. *Int. J. Chem. Kinet.* **1995**, *27*, 261–275.

- (23) Prinn, R. G.; Weiss, R. F.; Miller, B. R.; Huang, J.; Alyea, F. N.; Cunnold, D. M.; Fraser, P. J.; Hartley, D. E.; Simmonds, P. G. *Science* **1995**, *269*, 187–192.
- (24) Hein, R.; Crutzen, P. J.; Heimann, M. *Global Biogeochem. Cycles* **1997**, *11*, 43–76.

Received for review August 11, 1999. Revised manuscript received November 16, 1999. Accepted December 6, 1999.

ES9909374